

Charge noise acting on graphene double quantum dots in circuit quantum electrodynamics architecture

Yan Li(李炎), Shu-Xiao Li(李舒啸), Hai-Ou Li(李海欧)dag, Guang-Wei Deng(邓光伟), Gang Cao(曹刚), Ming Xiao(肖明), Guo-Ping Guo(郭国平)

Citation: Chin. Phys. B . 2018, 27(7): 076105. **doi:** 10.1088/1674-1056/27/7/076105

Journal homepage: http://cpb.iphy.ac.cn; http://iopscience.iop.org/cpb

What follows is a list of articles you may be interested in

Facile and controllable synthesis of molybdenum disulfide quantum dots for highly sensitive and selective sensing of copper ions

Xue Li(李雪), Da-Wei He(何大伟), Yong-Sheng Wang(王永生), Yin Hu(胡音), Xuan Zhao(赵宣), Chen Fu(付晨), Jing-Yan Wu(吴静燕)

Chin. Phys. B . 2018, 27(5): 056104. **doi:** 10.1088/1674-1056/27/5/056104

Preparation of graphene oxides with different sheet sizes by temperature control

Zhe Qian(钱哲), Liang Chen(陈亮), De-Yuan Li(李德远), Bing-Quan Peng(彭兵权), Guo-Sheng Shi(石国升), Gang Xu(徐刚), Hai-Ping Fang(方海平), Ming-Hong Wu(吴明红)

Chin. Phys. B . 2017, 26(10): 106101. **doi:** 10.1088/1674-1056/26/10/106101

Label-free tungsten disulfide quantum dots as a fluorescent sensing platform for highly efficient detection of copper (II) ions

Xuan Zhao(赵宣), Da-Wei He(何大伟), Yong-Sheng Wang(王永生), Yin Hu(胡音), Chen Fu(付晨), Xue Li(李雪)

Chin. Phys. B . 2017, 26(6): 066102. **doi:** 10.1088/1674-1056/26/6/066102

Photoconductive multi-layer graphene photodetectors fabricated on etched silicon-on-insulator substrates

Yu-Bing Wang(王玉冰), Wei-Hong Yin(尹伟红), Qin Han(韩勤), Xiao-Hong Yang(杨晓红), Han Ye(叶焓), Qian-Qian Lv(吕倩倩), Dong-Dong Yin(尹冬冬)

Chin. Phys. B . 2017, 26(2): 028101. **doi:** 10.1088/1674-1056/26/2/028101

Growth of PbS nanoclusters on specific sites of programmed oligodeoxynucleotides

Lu Ying, Teng Cui-Juan, Li Ying, Wang Hui, Xu Chun-Hua, Hu Shu-Xin, Li Ming

Chin. Phys. B . 2015, 24(1): 016101. **doi:** 10.1088/1674-1056/24/1/016101

RAPID COMMUNICATION

Charge noise acting on graphene double quantum dots in circuit quantum electrodynamics architecture*

Yan Li(李炎), Shu-Xiao Li(李舒啸), Hai-Ou Li(李海欧)†, Guang-Wei Deng(邓光伟), Gang Cao(曹刚), Ming Xiao(肖明), and Guo-Ping Guo(郭国平)‡

CAS Key Laboratory of Quantum Information, University of Science and Technology of China, Hefei 230026, *China*

(Received 10 March 2018; revised manuscript received 10 April 2018; published online 25 June 2018)

We investigate the dephasing mechanisms induced by the charge noise and microwave heating effect acting on a graphene double quantum dot (DQD) capacitively coupled to a microwave resonator. The charge noise is obtained from DC transport current, and its contribution to dephasing is simultaneously determined by the amplitude response of the microwave resonator. A lowfrequency $1/f$-type noise is demonstrated to be the dominant factor of the dephasing of graphene DQD. Furthermore, when the applied microwave power is larger than −90 dBm, the dephasing rate of graphene DQD increases rapidly with the increase of microwave power, and fluctuates slightly with the applied microwave power smaller than −90 dBm. Our results can be applied to suppress the impeditive influence on the dephasing of graphene-based devices associated with microwave input in the perspective investigations.

Keywords: quantum dot, microwave resonator, charge noise, graphene

PACS: 61.48.Gh, 68.65.Hb, 03.67.Lx, 85.40.Qx **DOI:** 10.1088/1674-1056/27/7/076105

In recent years, combining the on-chip microwave resonators and gate-defined quantum dots (QDs) in circuit quantum electrodynamics (cQED) architectures have attracted considerable attention.[1] Such hybrid QD-resonator devices have been realized on a variety of materials. QDs are considered as promising candidates for quantum information processing, and microwave resonators are used for sensitive metrology[2–8] or mediating multiple QDs for scalability.[9–12] Moreover, strong coupling regime is an important milestone in cQED systems, indicating that the coupling strength exceeds dephasing rate and photon loss rate.[13,14] Very recently, a strong charge-resonator coupling has been realized on GaAs,[2] Si,[3] and carbon nanotube,[4] and strong spin-resonator coupling has got extraordinary breakthroughs on Si[5,6] and GaAs.[7]

Graphene has also obtained impressive attention due to its interesting physical properties and promising applications. However, strong coupling between resonator and charge or spin has not been achieved in graphene system. One crucial challenge is to control over the dephasing rate,[15–19] which is the key indicator calibrating whether a physical system can act as a qubit.[20] Charge noise and microwave heating effect are the well-known sources of dephasing of qubits.[21–26] In GaAs system, the previous experiment has manifested that the $1/f$-type charge noise is the main contributor of dephasing.[27] So far, numerous studies have focused on the charge noise in different graphene-based devices.[28–30] However, in the hybrid graphene double quantum dot (DQD)-resonator architecture, there has been no reports on charge noise and microwave heating effect as well as their influences on the dephasing of graphene DQD up to now.

In this paper, we employ the graphene DQD-resonator hybrid device to extract $1/f$-type charge noise and white noise in the environment surrounding the graphene DQD. Furthermore, we evaluate the dephasing mechanisms of graphene DQD affected by the charge noise and microwave heating effect. It is demonstrated that $1/f$ noise is the dominant factor of dephasing in graphene DQD-resonator system, and the dephasing rate of graphene DQD increases rapidly when the microwave power applied in the resonator is larger than −90 dBm.

As exhibited in Fig. 1(a), the hybrid device consists of a superconducting half-wavelength refection line resonator (RLR)[33,34] and two graphene DQDs. Figure 1(b) shows the typical structure of graphene DQD and adjacent quantum point contact (QPC) channel. Source (S_D) and drain (D_D) are used to drive the current through DQD, and two depletion gates (G_1, G_2) are applied to tune the chemical potential of the DQD. S_Q, D_Q, and G_Q are used for the separated QPC. Each graphene DQD is capacitively coupled to the superconducting differential stripline of the resonator via its source lead. The two differential striplines of resonator are respectively coupled to input and output ports via finger capacitors. The sample is mounted on the dry dilution refrigerator with the base temper-

*Project supported by the National Key Research and Development Program of China (Grant No. 2016YFA0301700), the National Natural Science Foundation of China (Grant Nos. 61674132, 11674300, 11575172, and 11625419), and the Anhui Initiative in Quantum information Technologies, China (Grant No. AHY080000). This work was partially carried out at the USTC Center for Micro and Nanoscale Research and Fabrication.

†Corresponding author. E-mail: haiouli@ustc.edu.cn

‡Corresponding author. E-mail: gpguo@ustc.edu.cn

© 2018 Chinese Physical Society and IOP Publishing Ltd

ature of 26 mK in order to isolate from thermal radiation of higher temperature stages inside the refrigerator. Figure 2(c) exhibits the circuit schematic and measurement setup. A continuous microwave signal is split into two differential signals by 180° hybrid and then applied into striplines, establishing a steady electromagnetic field. The DQDs are positioned at the antinodes of electromagnetic field. The variations of DQD states would influence the electromagnetic field and thus lead to the shifts in amplitude and phase of the reflected microwave signal. Finally, the reflected signal is measured by the network analyzer after a primary cryogenic amplifier and a series of secondary room-temperature amplifiers.

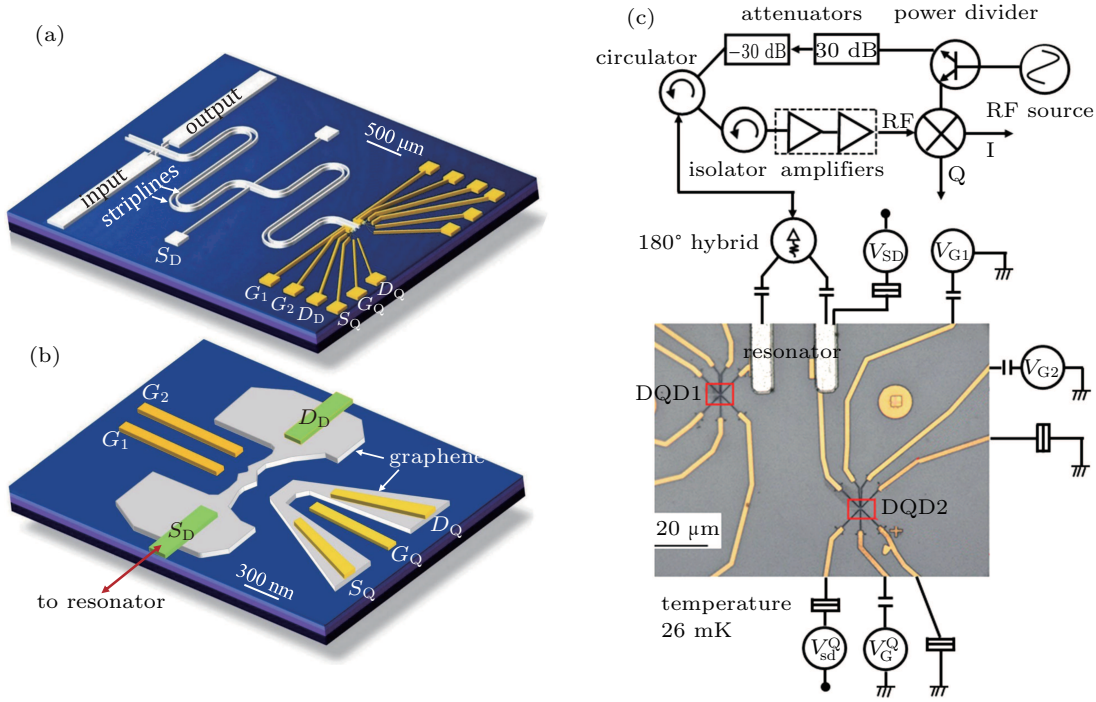


Fig. 1. (a) Circuit schematic of the hybrid device. The cavity (white) consists of two differential strip lines. The AC pads are used for the input and output of microwave. The two graphene DQDs are coupled to the resonator by source leads. (b) The typical structure of DQD and adjacent QPC channel, which are made of few-layer graphene flakes. (c) Circuit schematic and measurement setup of the hybrid device.

Firstly, we modulated the chemical potential of graphene DQD by tuning gates voltage. The DC transport current through DQD was recorded as a function of V_{G1} and V_{G2}. A typical hexagon-shaped charge stability diagram of DQD was observed,[2–4,35–37] as plotted in Fig. 2(a). In order to calibrate the lever arm of each gates, the DC signal was measured along the red dashed arrow indicated in Fig. 2(a). In this process, the energy level in the right dot was modified but energy level in left dot remained unchanged. As a consequence, we obtained the Coulomb diamond, from which the charging energy of the system is determined to be $E_C \sim 1.7$ meV, as shown in Fig. 2(b).

Secondly, we characterized the microwave resonator and then employed the resonator to probe the charge states of the graphene DQD. The amplitude and phase responses would be affected by the dispersive and dissipative coupling between QDs and resonator. The amplitude (A) of the resonator was extracted from the reflected microwave responses by the network analyzer, as plotted in the inset of Fig. 2(d). The characteristic parameters of the resonator can be determined from the $\lambda/2$ open-circuit microstrip resonator model[10,15,32] based on the input-output theory.[38] The resonance frequency of the bare resonator is determined to be $\omega_0/2\pi = 6.35$ GHz. The internal loss is $\kappa_i/2\pi = 0.68$ MHz and external loss is $\kappa_e/2\pi = 1.32$ MHz. The quality factor is ~ 3100.

In the following, we chose DC transport as the detecting channel to analyze the charge noise. Simultaneously, the dephasing rate[10,16,38] of graphene DQD is determined by the amplitude response of RLR with −96 dBm microwave power applied. Sweeping along detuning line (black solid arrow) in Fig. 2(a), the charge is shifted from the left dot to the right dot, we obtained the transport current and differential conductance as functions of ε, as plotted in Fig. 2(c).

In the meanwhile, we recorded the amplitude response as a function of ε, as plotted in Fig. 2(d). The dephasing rate $\gamma_\varphi/2\pi$ of graphene DQD can be extracted from the reflection coefficient $S_{21}(\omega)$,[38] which is the typical model used to describe DQD resonators in various materials[10,15,16]

$$S_{21}(\omega) = -\frac{j(\omega_0-\omega)+\dfrac{g_c^2}{j(\Omega-\omega)+\gamma_\varphi}+\dfrac{1}{2}(\kappa_i-\kappa_e)}{j(\omega_0-\omega)+\dfrac{g_c^2}{j(\Omega-\omega)+\gamma_\varphi}+\dfrac{1}{2}(\kappa_i+\kappa_e)}. \quad (1)$$

The amplitude is determined as $A = \mid S_{21}(\omega) \mid$, where g_c is the DQD-resonator coupling strength, and $\Omega = \sqrt{({2t_c}^2+\varepsilon^2)}$ and $2t_c$ are the tunneling energy. By fitting the experimental amplitude to the reflection coefficient, we extracted that the total dephasing of DQD is $\gamma_\varphi/2\pi = 1.59$ GHz, $g_c/2\pi = 21$ MHz, and $2t_c/2\pi = 7.3$ GHz.

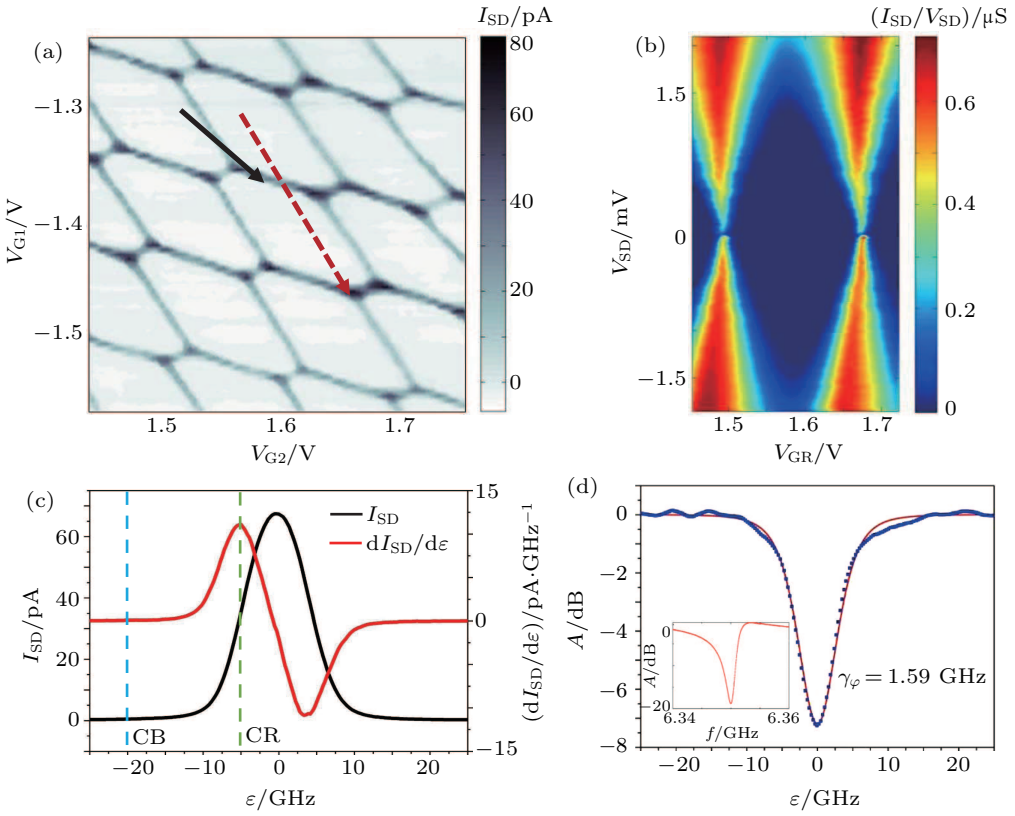


Fig. 2. (color online) (a) Charge stability diagram of DQD measured by DC transport current. Red dashed line is the sweeping direction to obtain the Coulomb diamond. Black solid arrow is the direction of sweeping detuning ε. (b) Coulomb diamond diagram obtained by sweeping along red dashed arrow in part (a). (c) Transport current (black line) and differential conductance curve (red line) of DQD sweeping detuning ε. Green and cyan dashed lines respectively indicate the Coulomb resonance (CR) position and Coulomb blockade (CB) position of charge noise. (d) Amplitude signal of the resonator as a function of ε. The blue dots are experimental data and the red line is a fitting curve with an extracted dephasing rate $\gamma_\varphi/2\pi = 1.59$ GHz. Inset: amplitude response of the resonator as a function of frequency, from which the characteristic parameters of the resonator can be determined.

To determine the charge noise spectral density of the environment in which the graphene DQD is surrounded, we measured the time traces of the transport current at two different detuning values, indicated as green and cyan dashed lines in Fig. 2(c). During the charge noise measurement, the time traces of transport current were acquired for 3704 s with the sampling time interval set at 0.1482 s. The recorded noise data of two detuning values are shown in Fig. 3(a). In order to get a relatively smooth power spectrum density (PSD), we use Bartlett method[39] and divide each data into five pieces, thus each piece contains 5000 points of total 25000 points. After PSD transform of each piece and then getting the average value of five pieces, thus we get the current PSD curve, as shown in Fig. 3(c). The cyan line, at Coulomb blockade (CB) position, only carries information about the intrinsic noise of the measurement setup and environment. The green curve, at Coulomb resonance (CR) position, is sensitive to charge fluctuations, containing both charge noise as well as intrinsic noise. Therefore, the difference between the upper green curve and the lower cyan curve in Fig. 3(c) reveals the influence of charge noise on transport current of the graphene DQD.

The charge noise PSD can be determined by the following equation:[27]

$$S_{\rm C}(\mathrm{e}^2/\mathrm{Hz}) = \left(\frac{e}{E_{\rm C}}\right)^2 \left(\frac{\partial\varepsilon}{\partial I}\right)^2 \Bigg|_{\varepsilon_{\rm sens}} (S_{\rm I}^{\rm CR} - S_{\rm I}^{\rm CB}). \quad (2)$$

The obtained result is shown in Fig. 3(d). Apparently, the charge noise PSD spectrum of DQD consists of two parts. One is a white noise floor at a higher frequency with a level of 3.9×10^{-5} e^2/Hz, and the other is a standard $1/f$ noise with a slope of $\sigma_{\rm C}^2 = 5.0\times10^{-5}$ e^2/Hz.[40–44] Correspondingly, we get the equivalent detuning fluctuation noise S_ε[45,46]

$$\begin{aligned} S_\varepsilon &= (E_{\rm C}/e)^2 S_{\rm C} = 65.0\ (\mu\mathrm{eV})^2/\mathrm{Hz} \\ &= 3.68\ (\mathrm{GHz})^2/\mathrm{Hz}. \end{aligned} \quad (3)$$

For comparison, the obtained S_ε in graphene DQD is on the same order of $S_\varepsilon = 57.1\ (\mu\mathrm{eV})^2/\mathrm{Hz}$ in GaAs-based DQD,[27] and $S_\varepsilon = 25.0\ (\mu\mathrm{eV})^2/\mathrm{Hz}$ in carbon nanotube-based DQD.[45]

Combining the experimental results with the second order semi-classical model for dephasing,[21,45,47] it is able to calculate the dephasing rate of the DQD contributed by detuning fluctuation noise as follows:[27,47–49]

$$\gamma_\varphi/2\pi = \frac{\mathrm{d}^2\Omega}{\mathrm{d}^2\varepsilon}\Big|_{\varepsilon=0} S_\varepsilon = S_\varepsilon/2t_{\rm c}. \quad (4)$$

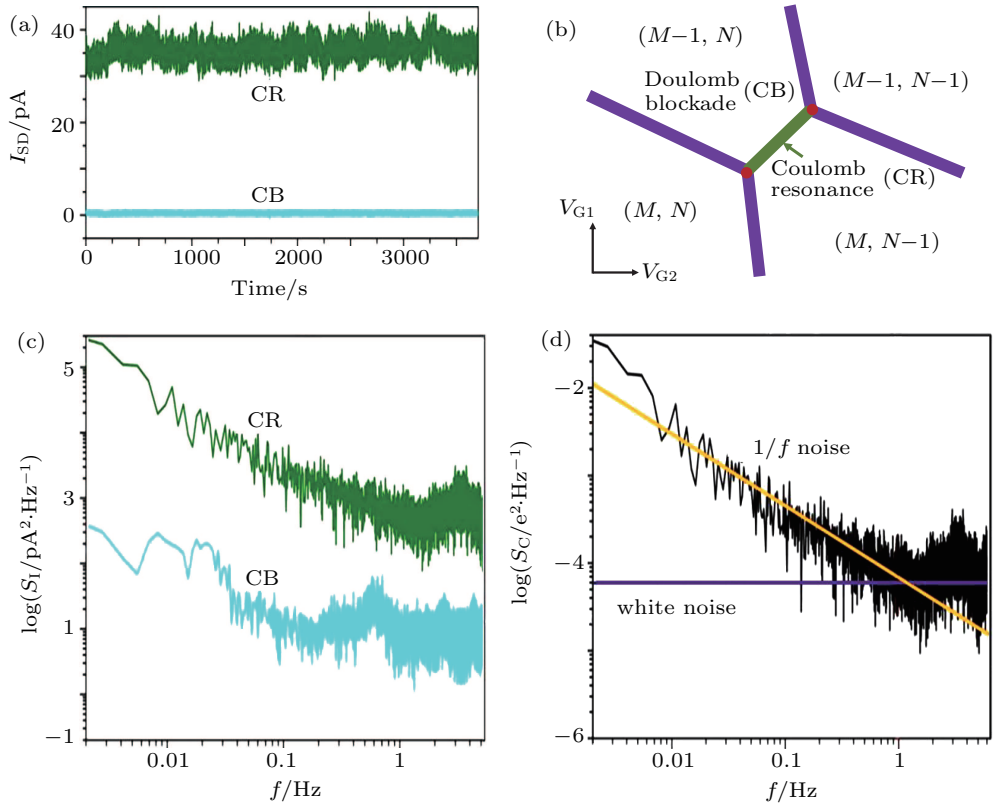


Fig. 3. (color online) (a) Time traces of DC transport current in the CR and CB positions, indicated as the green and cyan lines in Fig. 2(c). (b) Schematic of the charging diagram of the DQD with CR and CB indicated. The (N,M) means the number of electrons in the left dot and right dot respectively. (c) Current noise spectrum calculated from the green and cyan curves in panel (a). (d) The whole spectrum of charge noise PSD consists of a $1/f$ noise (orange line) and a white noise (yellow line). The microwave power applied in RLR is −96 dBm.

Therefore, with −96 dBm microwave power applied, the dephasing rate contributed by $1/f$ charge noise can be evaluated to be $\gamma_\varphi^C/2\pi \approx 1.06$ GHz, which contributes the main part of the total dephasing rate $\gamma_\varphi/2\pi = 1.59$ GHz of the graphene DQD. This result demonstrates that $1/f$ noise is the dominant source of dephasing in the graphene DQD-resonator system at low frequency.

Furthermore, previous studies have demonstrated that the graphene DQD absorbs microwave power easily, especially at resonance, leading to the increasing transport current due to the electron heating by the resonator microwave field.[10] In the meanwhile, charges inside the DQD are motivated with enough energy to tunnel through a series of puddles formed in graphene etched nanostructures, thus leading to the increase of $1/f$ noise.[30,40,50] In the following, we focus on the microwave heating effect and its effect on the dephasing of graphene DQD. With the different microwave power applied, the charge noise is measured by the DC transport current, and the amplitude of RLR is simultaneously recorded to extract the dephasing rate.

Figure 4(a) shows the transport current variation as a function of the applied microwave power (P). The value of DC transport current through the DQD with power $P = -85$ dBm is nearly twice as large as that with $P = -94$ dBm. The standard deviation changes of the DC current with $P = -85$ dBm is almost four times as large as that with $P = -94$ dBm. Figures 4(b) and 4(c) show the measured charge noise PSD and extracted dephasing rate γ_φ of graphene DQD with three microwave power (−94 dBm, −91 dBm, and −85 dBm). With the increase of microwave power, increasing tendencies are observed in both S_C and γ_φ, indicating that graphene DQD suffers a heavy microwave heating effect.[10,40] Note that unavoidable additional structures occur around 3.5 Hz may result from either a periodic charge noise in the host material or the measurement setup fluctuations leading to detuning noise.[27] Then we repeat the measurements of S_C and γ_φ with P which ranges from −96 dBm to −84 dBm in steps of 1 dBm, as shown in Fig. 4(d). When microwave power $P < -90$ dBm (blue region), γ_φ shows a slight fluctuation with increasing P. However, when $P > -90$ dBm (yellow region), γ_φ increases rapidly with the increase of microwave power.

Notably, various experimental studies based on graphene need the applied microwave power much larger than −90 dBm, such as photon-assisted tunneling (PAT),[51] With the large microwave power applied, the expected PAT phenomenon may be submerged in thermal noise or rapidly disappeared due to short dephasing time. We believe our finding is of crucial importance in the design of graphene-based systems associated with microwave input. The applied microwave power should be less than −90 dBm in our measurement setup, or the dephasing of the system could be greatly influenced.

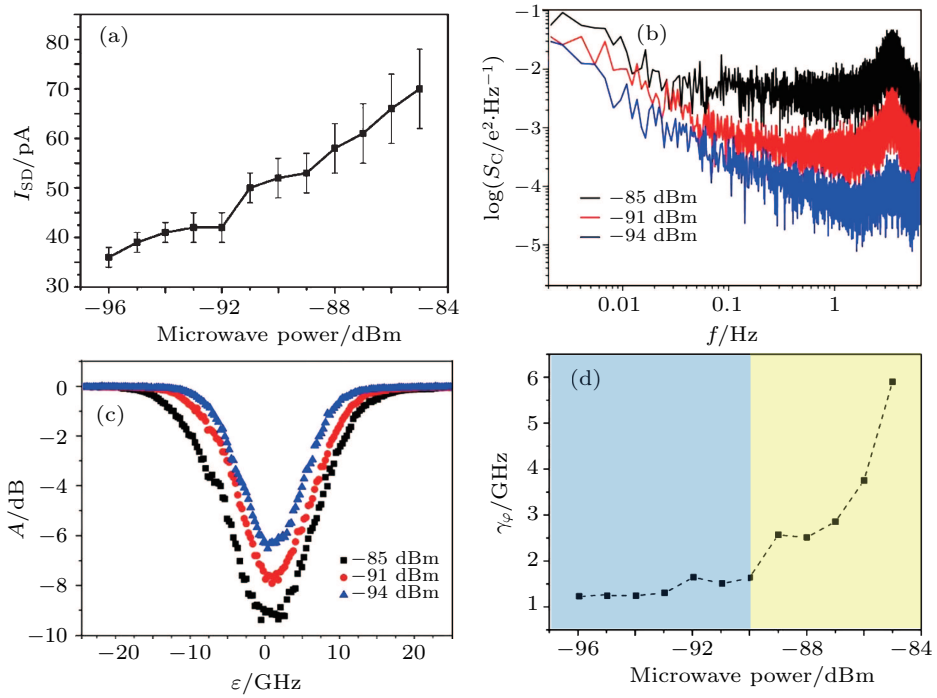


Fig. 4. (color online) (a) Transport current in sensitive position as a function of microwave power applied to RLR. Current signal as well as its noise (shown as the error bar) increases with microwave power. (b) Charge noise PSD with different microwave power. Noise exhibits the increasing tendency with the increase of microwave power. (c) Amplitude signal of the resonator as a function of ε with different microwave power. (d) The related dephasing rate γ_φ versus applied microwave power extracted from amplitude signal of the RLR. It shows a slight fluctuation with microwave power below −90 dBm and a rapid increase with microwave power above −90 dBm.

In conclusion, we investigate the dephasing mechanisms of graphene DQD affected by the charge noise and microwave heating effect in the hybrid architecture which consists of a graphene DQD and a capacitively coupled microwave resonator. The charge noise is obtained from DC transport current, and its contribution to dephasing is simultaneously determined by the amplitude response of the microwave resonator. In the graphene DQD-resonator system, the low-frequency $1/f$-type charge noise is demonstrated to be the dominant factor of the dephasing of graphene DQD. Furthermore, when the microwave power applied in the resonator is larger than −90 dBm, the dephasing rate of graphene DQD increases rapidly with the increase of microwave power, and fluctuates slightly with the microwave power smaller than −90 dBm. We anticipate our work would be important for the design of graphene-based systems associated with microwave input.

References

[1] Xiang Z L, Ashhab S, You J Q and Nori F 2013 *Rev. Mod. Phys.* **85** 623

[2] Stockklauser A, Scarlino P, Koski J V, Gasparinetti S, Andersen C K, Reichl C, Wegscheider W, Ihn T, Ensslin K and Wallraff A 2017 *Phys. Rev. X* **7** 011030

[3] Mi X, Cady J V, Zajac D M, Deelman P W and Petta J R 2017 *Science* **355** 156

[4] Bruhat L E, Cubaynes T, Viennot J J, Dartiailh M C, Desjardins M M, Cottet A and Kontos T 2016 arXiv:161205214

[5] Mi X, Benito M, Putz S, Zajac D M, Taylor J M, Burkard G and Petta J R 2018 *Nature* **555** 599

[6] Samkharadze N, Zheng G, Kalhor N, Brousse D, Sammak A, Mendes U C, Blais A, Scappucci G and Vandersypen L M K 2018 *Science* **359** 1123

[7] Landig A J, Koski J V, Scarlino P, Mendes U C, Blais A, Reichl C, Wegscheider W, Wallraff A, Ensslin K and Ihn T 2017 arXiv:171101932

[8] Han T Y, Deng G W, Wei W and Guo G P 2016 *Chin. Phys. Lett.* **33** 047301

[9] Delbecq M R, Bruhat L E, Viennot J J, Datta S, Cottet A and Kontos T 2013 *Nat. Commun.* **4** 1400

[10] Deng G W, Wei D, Li S X, Johansson J R, KongW C, Li H O, Cao G, Xiao M, Guo G C, Nori F, Jiang H W and Guo G P 2015 *Nano Lett.* **15** 6620

[11] Liu B Y, Cui W, Dai H Y, Chen X and Zhang M 2017 *Chin. Phys. B* **26** 090303

[12] Zhu Z C, Tu T and Guo G P 2011 *Chin. Phys. Lett.* **28** 040301

[13] Hu X D, Liu Y X and Nori F 2012 *Phys. Rev. B* **86** 035314

[14] Jin P Q, Marthaler M, Shnirman A and Schön G 2012 *Phys. Rev. Lett.* **108** 190506

[15] Deng G W, Wei D, Johansson J R, Zhang M L, Li S X, Li H O, Cao G, Xiao M, Tu T, Guo G C, Jiang H W, Nori F and Guo G P 2015 *Phys. Rev. Lett.* **115** 126804

[16] Volk C, Neumann C, Kazarski S, Fringes S, Engels S, Haupt F, Muller A and Stampfer C 2013 *Nat. Commun.* **4** 1753

[17] Zhang K, Li M M, Liu Q, Yu H F and Yu Y 2017 *Chin. Phys. B* **26** 078501

[18] Zhang X, Li H O, Wang K, Cao C, Xiao M and Guo G P 2018 *Chin. Phys. B* **27** 020305

[19] Su F F, Liu W Y, Xu H K, Deng H, Li Z Y, Tian Y, Zhu X B, Zheng D N, Lv L and Zhao S P 2017 *Chin. Phys. B* **26** 060308

[20] Huang P H and Hu X D 2014 *Phys. Rev. B* **89** 195302

[21] Petersson K D, Petta J R, Lu H and Gossard A C 2010 *Phys. Rev. Lett.* **105** 246804

[22] Dupont-Ferrier E, Roche B, Voisin B, Jehl X, Wacquez R, Vinet M, Sanquer M and Franceschi S D 2013 *Phys. Rev. Lett.* **110** 136802

[23] Dial O E, Shulman M D, Harvey S P, Bluhm H, Umansky V and Yacoby A 2013 *Phys. Rev. Lett.* **110** 146804

[24] Paladino E, Galperin Y M, Falci G and Altshuler B L 2014 *Rev. Mod. Phys.* **86** 361

[25] Adam B, Daniel K and Dimitrie C 2014 *Appl. Phys. Lett.* **105** 192102

[26] Yu S X, Lai C H and Oh C H 2011 *Acta Phys. Sin.* **60** 050304 (in Chinese)

[27] Basset J, Stockklauser A, Jarausch D D, Frey T, Reichl C, Wegscheider W, Wallraff A, Ensslin K and Ihn T 2014 *Appl. Phys. Lett.* **105** 063105

[28] Xu G Y, Torres C M, Song E B, Tang J S, Bai J W, Duan X F, Zhang Y G and Wang K L 2010 *Nano Lett.* **10** 4590

[29] Cheng Z G, Li Q, Li Z J, Zhou Q Y and Fang Y 2010 *Nano Lett.* **10** 1864

[30] Song X X, Li H O, You J, Han T Y, Cao G, Tu T, Xiao M, Guo G C, Jiang H W and Guo G P 2015 *Sci. Rep.* **5** 8142

[31] Zhang M L, Deng G W, Li S X, Li H O, Cao G, Tu T, Xiao M, Guo G C, Jiang H W, Siddiqi I and Guo G P 2014 *Appl. Phys. Lett.* **104** 083511

[32] Li Y, Li S X, Gao F, Li H O, Xu G, Wang K, Liu D, Cao G, Xiao M, Wang T, Zhang J J, Guo G C and Guo G P 2018 *Nano Lett.* **18** 2091

[33] Pozar D M 2004 *Microwave Engineering* (Wiley)

[34] Petersson K D, McFaul L W, Schroer M D, Jung M, Taylor J M, Houck A A and Petta J R 2012 *Nature* **490** 380

[35] Zhou C, Wang L, Tu T, Han T Y, Li H O and Guo G P 2013 *Chin. Phys. Lett.* **30** 050301

[36] Zhou C, Tu T, Wang L, Li H O, Cao G, Guo G C and Guo G P 2012 *Chin. Phys. Lett.* **29** 117303

[37] Wang L J, Cao G, Tu T, Li H O, Zhou C, Hao X J, Guo G C and Guo G P 2011 *Chin. Phys. Lett.* **28** 067301

[38] Tavis M and Cummings F W 1968 *Phys. Rev.* **170** 379

[39] Rahi P K and Mehra R 2013 *Int. J. Sci. Res. Eng. Tech.* **2** 389

[40] Li H O, Cao G, Xiao M, You J, Wei D, Tu T, Guo G C, Jiang H W and Guo G P 2014 *J. Appl. Phys.* **116** 174504

[41] Culcer D, Hu X D and Sarma S D 2009 *Appl. Phys. Lett.* **95** 073102

[42] Dial O, Shulman M, Harvey S, Bluhm H, Umansky V and Yacoby A 2013 *Phys. Rev. Lett.* **110** 146804

[43] Martin I and Galperin Y M 2006 *Phys. Rev. B* **73** 180201

[44] Jung S W, Fujisawa T, Hirayama Y and Jeong Y H 2004 *Appl. Phys. Lett.* **85** 768

[45] Viennot J J, Delbecq M R, Dartiailh M C, Cottet A and Kontos T 2014 *Phys. Rev. B* **89** 165404

[46] Petersson K D, Petta J R, Lu H and Cossard A C 2010 *Phys. Rev. Lett.* **105** 246804

[47] Ithier G, Collin E, Joyez P, Meeson P J, Vion D, Esteve D, Chiarello F, Shnirman A, Makhlin Y, Schriefl J and Schoen G 2005 *Phys. Rev. B* **72** 134519

[48] Dutta P and Horn P M 1981 *Rev. Mod. Phys.* **53** 497

[49] Paladino E, Faoro L, Falci G and Rosario F 2002 *Phys. Rev. Lett.* **88** 228304

[50] Gallagher P, Tod K and Goldhaber-Gordon D 2010 *Phys. Rev. B* **81** 115409

[51] You J, Li H O, Cao G, Deng G W, Xiao M and Guo G P 2015 *Europhys. Lett.* **111** 17001